

Strain-induced scrolling of Janus WSSe

Yanlin Gao ^{1,*}, Masahiko Kaneda,² Takahiko Endo,² Hiroshi Nakajo,^{3,4,5} Soma Aoki,^{3,4} Toshiaki Kato ^{3,4},
Yasumitsu Miyata ² and Susumu Okada ¹

¹*Department of Physics, Graduate School of Science and Technology, University of Tsukuba,
1-1-1 Tennodai, Tsukuba, Tsukuba 305-8571, Japan*

²*Department of Physics, Tokyo Metropolitan University, Hachioji 192-0397, Japan*

³*Graduate School of Engineering, Tohoku University, Sendai 980-8579, Japan*

⁴*Advanced Institute for Materials Research (AIMR), Tohoku University, Sendai 980-8577, Japan*

⁵*Kokusai Electric Corporation, Toyama 939-2393, Japan*



(Received 13 October 2023; revised 18 June 2024; accepted 26 June 2024; published 11 July 2024)

Employing density functional theory, we explore the energetics, geometries, and electronic properties of Janus WSSe in terms of curvature effects. Total energy calculations on tubular forms of Janus WSSe reveal that Janus WSSe intrinsically possesses a scrolled conformation with a radius of curvature of 2.3 nm or larger. Scrolling releases compressive and tensile strains on the Se and S atoms, respectively, in the flat conformation. Curvature associated with scrolling does not affect the band edge alignment of the Janus WSSe. The internal electric field across a WSSe layer decreases monotonically with increasing curvature.

DOI: [10.1103/PhysRevB.110.035414](https://doi.org/10.1103/PhysRevB.110.035414)

I. INTRODUCTION

In the field of material sciences, atomic-layer materials have triggered a paradigm shift because they can form various derivatives that are unavailable by conventional synthetic procedures [1]. Their two-dimensional covalent networks with chemically inert surfaces enable various out-of-plane derivatives in which interlayer spacing plays a crucial role in determining their physical properties and causes unusual phenomena that are absent in the conventional bulk systems [2–23]. In addition, they can form in-plane derivatives through the selection of appropriate combinations of constituent elements that possess similar ionic radii and valence [14,21,22]. The electronic properties of these derivatives exceed a simple superposition of those of the constituent atomic-layer materials. Indeed, most transition metal dichalcogenide (TMD) monolayers change their band edge alignment from a direct to an indirect band gap by forming bilayer or multilayer structures [24,25]. Furthermore, out-of-plane derivatives of TMDs possess unique band edge alignments depending on the constituent TMD and the external electric field [18,19]. The borders on the in-plane derivatives lead to border localized states and band bending that depend on the constituent layer materials and their atomic arrangement on the border [8,14,23,26]. By controlling the heterostructures and excess carriers, out-of-plane and in-plane derivatives of TMDs support transdimensional electron systems [27].

With three-atom-thick covalent networks composed of transition metals and chalcogen layers, TMDs can form a unique class of derivatives. The atomic layer of the transition metals arranged in the form of a triangular lattice is

sandwiched between two atomic layers consisting of different chalcogen elements arranged in a prismatic manner with a thickness of approximately 3 Å. The unique derivatives of TMDs are known as Janus TMDs because of their asymmetric chalcogen layers with respect to the transition metal atom layer. These Janus TMDs have been synthesized by sulfurization or selenization of one of the chalcogen layers of MSe_2 or MS_2 , for which M denotes a transition metal atom [28–32]. Structural asymmetry with respect to the transition metal layer leads to an internal electric field across the layers that causes Rashba spin splitting [33,34], remarkable photocatalytic effects [35–37], and the creation of stable excitons [38]. The asymmetry was expected to establish unique structures in Janus TMDs such as tubular, scrolled, and corrugated structures. Indeed, several theoretical works pointed out that the Janus TMDs possess the tubular structure as their ground-state conformation. Evarestov *et al.* demonstrated that the WSSe nanotube with an outer wall of Se atoms and a diameter of 4 nm possesses negative total energy with respect to the WSSe with a planar conformation [39]. MoSSe with an outer wall of Se atoms was reported to be more stable than a planar MoSSe ribbon [40]. Oshima *et al.* extrapolated that the MoSSe nanotube possesses the ground state with a diameter of 40 Å [41]. Despite these works pointing out the stabilities of a tubular structure of Janus TMD, direct numerical calculations around the energy minima are mandatory to give a quantitative discussion about the energetics and geometries of WSSe nanoscrolls.

In this paper, we aim to investigate the energetically stable conformation of Janus WSSe using density functional theory (DFT) along with the generalized gradient approximation (GGA). Our total-energy calculations reveal that an isolated monolayer Janus WSSe has a tubular or scrolled structure with radius of curvature of 2.3 nm or larger. Therefore,

*Contact author: ylgao@comas-tsukuba.jp

intrinsically, the WSSe or any other Janus TMD exhibits a tubular or scrolled conformation as the ground state. The tubular form decreases the compressive and tensile strains of the W-Se and W-S bonds, respectively, in planar WSSe. Our theoretical investigation of the electronic properties reveals that the band edge alignment and gap energy retain those of a flat conformation for tubular WSSe of radius 1.75 nm or larger. Moreover, the tubular structure substantially decreases the internal electric field across the layers.

II. METHODS

Geometric and electronic structures of Janus WSSe have been investigated within the framework of DFT [42,43] implemented in the Simulation Tool for Atom Technology (STATE) package [44]. We used the GGA with the Perdew-Burke-Ernzerhof functional to express the exchange-correlation potential between the interacting electrons [45]. The interactions between valence electrons and ions were described by ultrasoft pseudopotentials generated using the Vanderbilt scheme [46]. Note that the calculations do not contain the spin-orbit coupling, so that the band splitting in the valence band edges is absent. The valence wave function and deficit charge density were expanded in terms of the plane-wave basis set with cutoff energies of 25 and 225 Ry, respectively.

These cutoff energies allow for discussing the relative stability of WSSe-related materials. To investigate curvature effects on the energetics of Janus WSSe, we chose the tubular WSSe with armchair chirality as a structural model for the scrolled, tubular, and corrugated Janus WSSe. As for the tube axis direction, we assumed a lattice parameter of 0.319 nm which was obtained using the optimum lattice parameter of planar WSSe. To investigate the energetics of isolated WSSe nanotubes, each nanotube is separated by 0.8 nm vacuum spacing with its adjacent periodic images. All atoms were fully optimized until the force acting on each atom was less than 0.005 Ry/Å under a fixed lattice parameter along the tube axis. Integrations over the Brillouin zone for the self-consistent electronic structure calculation were performed using 5-*k* meshes along the axis of the tube.

Janus WSSe monolayers were prepared by the plasma-assisted surface atom substitution of WSe₂ monolayers [30,47] which were synthesized by chemical vapor deposition on SiO₂/Si substrates with WO₃ powder and Se granules as the precursors [48]. The Janus monolayers were then transformed into scrolls through spin-coating of chloroform solution. A cross-sectional transmission electron microscope (TEM) image was prepared using the focused ion beam method. TEM images were taken at an acceleration voltage of 200 kV using a high-resolution TEM (Hitachi High Technologies Corporation, H-9500). Details of sample preparation and characterization are reported elsewhere [49].

III. RESULTS AND DISCUSSION

Figure 1(a) shows the total energy per atom of the WSSe nanotube relative to that of flat WSSe as a function of tube diameter. The total energy of the WSSe tubes with outer walls of Se and S atoms decreases monotonically with increasing diameter within a small diameter region as for that of carbon

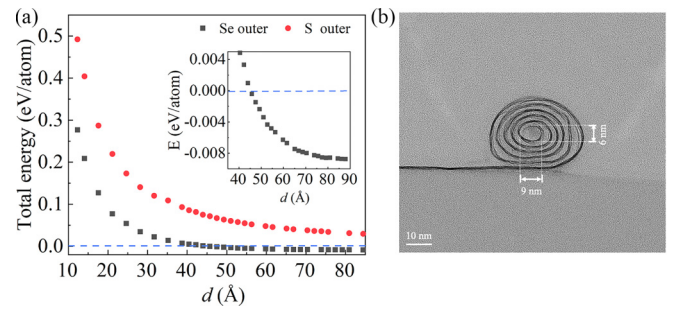


FIG. 1. (a) Total energy of Janus WSSe nanotubes with outermost walls of Se atoms and of S atoms as a function of diameter. The energy is measured relative to that of an isolated flat monolayer WSSe. (b) Cross-sectional TEM image of an experimentally obtained WSSe scroll with the outermost wall of Se atoms.

nanotubes and other TMD nanotubes [50–54]. For tubes with an outer wall of Se atoms, the total energy of tubes with diameters 4.6 nm or larger is lower than that of an isolated flat WSSe sheet, which is consistent with the result in the previous calculation [39]. The energy is approximately extrapolated by a polynomial of $1/r$,

$$E = 57.156 \left(\frac{1}{r}\right)^4 - 49.128 \left(\frac{1}{r}\right)^3 + 22.470 \left(\frac{1}{r}\right)^2 - 0.8976 \left(\frac{1}{r}\right),$$

where r is the radius of the Janus TMD nanotube. By using this function, we found that the total energy has a minimum value of approximately -9.0 meV at a diameter of 9.2 nm and asymptotically approaches zero corresponding to the energy of an isolated Janus WSSe sheet. The energy minimum of the WSSe tube is larger than that of the Janus MoSSe tube given in previous calculations [40,41], owing to the different optimal spacing between transition metal and chalcogen atoms. Our results indicate that the curved structure of WSSe with an outer wall of Se atoms is more stable than the flat WSSe for a wide range of diameters from 4.6 nm upward. Thus, Janus WSSe tends to possess tubular, scrolled, or a corrugated structure as its ground-state conformation. In particular, the scrolled conformation is the most plausible because the inter-wall van der Waals interaction further stabilizes the scrolled WSSe. In this case, the diameter of the innermost shell must be larger than 4.6 nm. Indeed, our TEM image indicates that the diameters of the innermost wall of the scrolled WSSe are approximately 9 nm and 6 nm for vertical and horizontal directions, respectively [Fig. 1(b)]. The gentle energy landscape around the minimum and the van der Waals binding energy between the WSSe shells make WSSe nanoscrolls the ground-state conformation of the WSSe, when it is peeled off the supporting substrates. In contrast, tubes with outer walls of S do not possess negative total energy with respect to that of the isolated flat WSSe. This result indicates that the WSSe scrolls with the outer walls of Se atoms are energetically stable.

To elucidate the physical origin of the energetic stability of the tubular or curved WSSe with an outer wall of Se atoms, we investigated the S-S and Se-Se distances along the circumference of the tubes in terms of the curvature (Fig. 2).

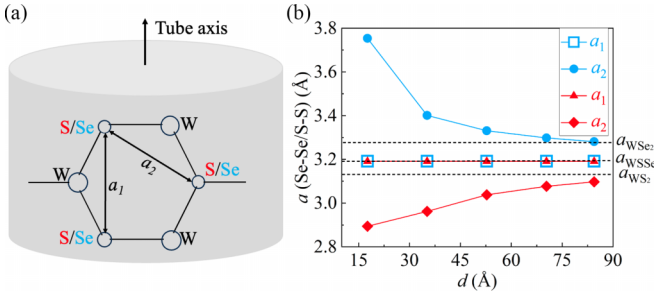


FIG. 2. (a) A schematic view of atomic arrangement along the circumference of armchair Janus WSSe tubes. (b) Distances between chalcogen atoms of Janus WSSe tubes of different diameters. The three dashed lines mark the values of the distances between chalcogen atoms in flat WSe_2 , WSSe, and WS_2 sheets, respectively. The gray-shaded cylinder represents a WSSe nanotube.

Those distances correspond to the lattice constant of the flat TMD with 1×1 unit so that they reflect the strains applied on S and Se surfaces of WSSe nanotubes. The S-S and Se-Se distances monotonically increase and decrease, respectively, with increasing the tube diameter. These distances are approximately the same as those of isolated flat WS_2 and WSe_2 , respectively, when the tubes had diameters of approximately 8.8 nm. These results indicate that compressive and tensile strains on S-W and Se-W bonds in tubular WSSe both substantially decrease when WSSe has curvatures of diameter of approximately 8.8 nm. Therefore, the optimum Se-Se and S-S spacings in WSSe tubes with large diameters are the physical origin that the Janus WSSe prefers the tubular form as its ground-state conformation. The strains on S and Se surfaces again increase with further increase of the tube diameter because the S-S and Se-Se distances along circumferences

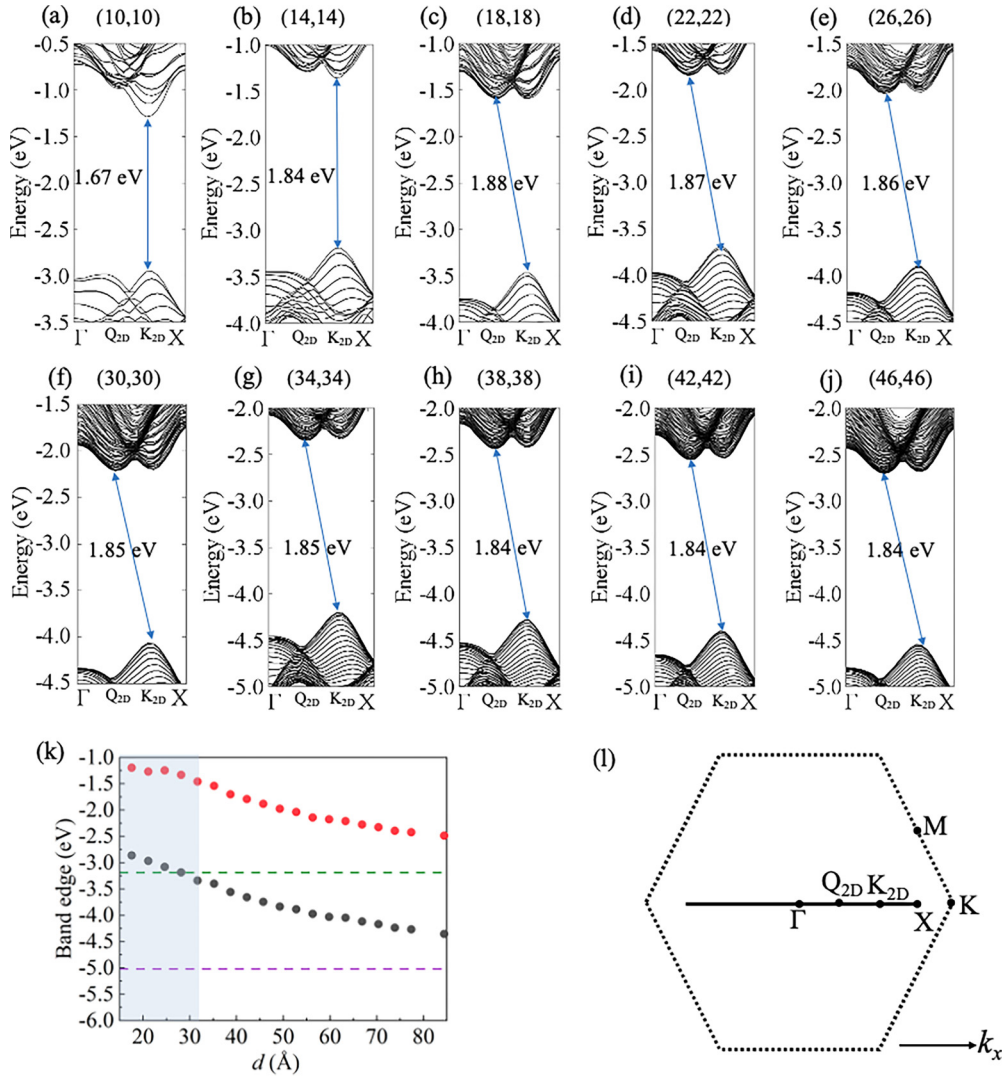


FIG. 3. Electronic structures of WSSe nanotubes with diameter of (a) 1.8, (b) 2.5, (c) 3.2, (d) 3.9, (e) 4.6, (f) 5.3, (g) 6.0, (h) 6.7, (i) 7.4, and (j) 8.1 nm. (k) Band edges of WSSe tubes with difference diameters. The black and red dots indicate the energy of the valence band top (VBT) and the conduction band bottom (CBB) of WSSe tubes, respectively. The purple and green dashed lines mark, respectively, VBT and CBB energies for flat WSSe. The shadow area corresponds to the WSSe tubes with the direct band gap. The energies are measured from the vacuum level outside the tubes. (l) Symmetry points in the first Brillouin zone of WSSe nanotube (a solid line) in which the symmetry points of the two-dimensional hexagonal Brillouin zone (a dotted hexagon) are also shown.

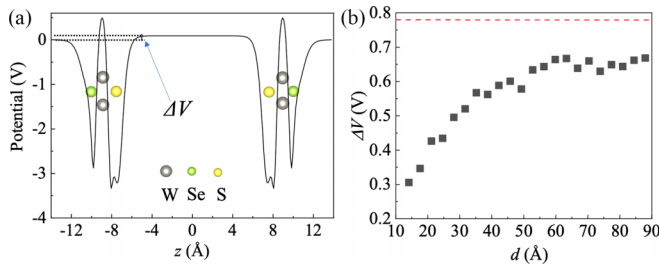


FIG. 4. (a) Electrostatic potential of a WSSe tube with the diameter 1.8 nm. (b) Electrostatic potentials of S atoms in the innermost wall relative to those in the outermost wall for WSSe tubes with different diameters. The red dashed line indicates the potential difference of flat WSSe.

asymptotically approach the optimum distance for the flat WSSe. Note that the Se-Se and S-S spacings along the tube axis are insensitive to the curvature value because the lattice parameter along the direction of the tube axis is fixed. Therefore, these facts indicate that the preferential orientation or chirality of nanoscrolls is expected to exist because all chalcogen spacings are relaxed for the tube with zigzag or near-zigzag chirality.

We investigate how curvature affects the electronic structure of Janus WSSe. Figures 3(a)–3(j) show the electronic structures of WSSe tubes. Note that the K and Q points of the hexagonal Brillouin zone are folded into the wave numbers at two-thirds and one-third of the Γ - X line, which are indicated as K_{2D} and Q_{2D} , respectively, because we are considering armchair WSSe tubes. The tubes with a diameter of 3.2 nm or less are semiconductor with direct band gap at the K_{2D} point, which corresponds to the K point of the hexagonal Brillouin zone. With increasing the tube diameter, the conduction band valley at the Q_{2D} point shifts downward and has almost the same energy as that at the K_{2D} point. The valley at the Q_{2D} point is deeper by 40 meV than that at the K_{2D} point. This band edge alignment is qualitatively the same as that of the isolated planar WSSe. Therefore, a scrolled or tubular WSSe possesses qualitatively the same electronic structure as a planar WSSe [37]. The band edge energy becomes deeper with decreasing curvature of the tubular structure. However, those are still shallower than those of an isolated WSSe sheet because of the strain effect in the WSSe tube with a diameter up to 8.8 nm, whose Se-Se and S-S distances along the circumference of the tube are still longer and shorter, respectively, than those of the isolated WSSe sheet [Fig. 3(k)]. It should be noted that the conduction band edge energies are underestimated because of the functional form for describing the exchange-correlation potential energy.

Figure 4(a) shows an electrostatic potential across the WSSe tube with a diameter of 1.8 nm. Similar to a flat WSSe, the potential at the S atom surface in the inner wall is higher than that of the Se atom surface in the outer wall, indicating an internal electric field across the layers. This internal electric field or the potential difference is weaker or smaller than that of a flat WSSe. Figure 4(b) gives the potential differences between the Se and S walls of the WSSe tube as

a functional of diameter along with the potential difference of flat WSSe indicated by a red dashed line. The potential difference is obtained from $\Delta V = V_{(0,0,c/2)} - V_{(0,0,0)}$, where c is the unit cell parameter normal to the axis of the tube. This potential difference is 0.34 V for a WSSe tube with a diameter of 1.8 nm, whereas it is 0.67 V for a tube with the diameter of 8.8 nm, indicating that the potential or internal electric field increases monotonically and approaches that of the flat WSSe (0.78 V) asymptotically with increasing diameter. Indeed, the potential differences for a WSSe tube with a diameter of 5.5 nm or larger are close to that of flat WSSe as shown in Fig. 4(b). However, the potential difference is still smaller than that of flat WSSe, because the tubes with the diameter of 8.8 nm still contain the tensile and compressive strains on S and Se surfaces compared with the flat WSSe. The decrease in the potential difference may deteriorate the physical and chemical functionalities of Janus TMD, such as catalytic activity and exciton stability. However, the stacking of multiple layers in a scrolled WSSe may prevent such deterioration because the total dipole moment across the walls is a simple superposition of the dipole moments of its constituent layers [55].

IV. SUMMARY

In summary, the energetics and electronic structures of Janus WSSe nanotubes were investigated using DFT. The total energy per atom of a WSSe nanotube relative to the monolayer decreases with increasing nanotube diameter; it is lower than that of isolated flat WSSe when the diameter is 4.6 nm or larger but saturates at -8 meV when the diameter is 6.8 nm. Therefore, intrinsically, Janus WSSe possesses a scrolled structure as its ground state without supporting substrates because the curvature releases the strain of Janus WSSe with an energy gain of up to 8 meV per atom. The Janus WSSe nanotubes with diameter less than 3.5 nm are semiconductors with direct band gaps at the K_{2D} point between the Γ and X points. However, nanotubes of diameter 3.5 nm or larger become indirect band gap semiconductors through the upward shift of the conduction band edge at the K_{2D} point. Furthermore, the electrostatic potential at the S surface of the innermost wall is higher than that at the Se surface of the outermost wall; however, the potential difference is smaller than that of monolayer flat WSSe.

ACKNOWLEDGMENTS

This work was supported by JST-CREST (Grants No. JPMJCR23A4 and No. JPMJCR23A2) from the Japan Science and Technology Agency, JSPS KAKENHI (Grants No. JP21H05233, No. JP21H05234, No. JP21H05232, No. JP20H05664, No. JP23H05469, No. JP22H00283, No. JP23H00097, No. JP23K17756, No. JP22H04957, and No. JP22H05441) from the Japan Society for the Promotion of Science, and the Joint Research Program on Zero-Emission Energy Research, Institute of Advanced Energy, Kyoto University. Parts of the calculations were performed on an NEC SX-Aurora at the Cybermedia Center at Osaka University.

- [1] H. Ago, S. Okada, Y. Miyata, K. Matsuda, M. Koshino, K. Ueno, and K. Nagashio, *Sci. Technol. Adv. Mater.* **23**, 275 (2022).
- [2] M. Koshino and E. McCann, *Phys. Rev. B* **80**, 165409 (2009).
- [3] M. Otani, M. Koshino, Y. Takagi, and S. Okada, *Phys. Rev. B* **81**, 161403(R) (2010).
- [4] T. Ohta, A. Bostwick, K. Horn, and E. Rotenberg, *Science* **313**, 951 (2006).
- [5] Y. Gao, M. Maruyama, and S. Okada, *Appl. Phys. Express* **13**, 065006 (2020).
- [6] Y. Gao and S. Okada, *Appl. Phys. Express* **14**, 035001 (2021).
- [7] Y. Cao, V. Fatemi, S. Fang, K. Watanabe, T. Taniguchi, and E. K. P. Jarillo-Herrero, *Nature (London)* **556**, 43 (2018).
- [8] S. Okada, M. Igami, K. Nakada, and A. Oshiyama, *Phys. Rev. B* **62**, 9896 (2000).
- [9] P. Rivera, J. R. Schaibley, A. M. Jones, J. S. Ross, S. Wu, G. Aivazian, P. Klement, K. Seyler, G. Clark, N. J. Ghimire, J. Yan, D. G. Mandrus, W. Yao, and X. Xu, *Nat. Commun.* **6**, 6242 (2015).
- [10] K. Zhang, T. Zhang, G. Cheng, T. Li, S. Wang, W. Wei, X. Zhou, W. Yu, Y. Sun, P. Wang, D. Zhang, C. Zeng, X. Wang, W. Hu, H. J. Fan, G. Shen, X. Chen, X. Duan, K. Chang, and N. Dai, *ACS Nano* **10**, 3852 (2016).
- [11] K. Wang, B. Huang, M. Tian, F. Ceballos, M.-W. Lin, M. Mahjouri-Samani, A. Boulesbaa, A. A. Puzos, C. M. Rouleau, M. Yoon, H. Zhao, K. Xiao, G. Duscher, and D. B. Geohegan, *ACS Nano* **10**, 6612 (2016).
- [12] D. Kozawa, A. Carvalho, I. Verzhbitskiy, F. Giustino, Y. Miyauchi, S. Mouri, A. H. C. Neto, K. Matsuda, and G. Eda, *Nano Lett.* **16**, 4087 (2016).
- [13] M. Z. Bellus, M. Li, S. D. Lane, F. Ceballos, Q. Cui, X. C. Zeng, and H. Zhao, *Nanoscale Horiz.* **2**, 31 (2017).
- [14] Y. Miyata, E. Maeda, K. Kamon, R. Kitaura, Y. Sasaki, S. Suzuki, and H. Shinohara, *Appl. Phys. Express* **5**, 085102 (2012).
- [15] A. K. Geim and I. V. Grigorieva, *Nature (London)* **499**, 419 (2013).
- [16] S. Masubuchi, M. Morimoto, S. Morikawa, M. Onodera, Y. Asakawa, K. Watanabe, T. Taniguchi, and T. Machida, *Nat. Commun.* **9**, 1413 (2018).
- [17] T. Yamaoka, H. E. Lim, S. Koirala, K. Shinokita, M. Maruyama, S. Okada, Y. Miyauchi, and K. Matsuda, *Adv. Funct. Mater.* **28**, 1801021 (2018).
- [18] M. Maruyama, K. Nagashio, and S. Okada, *ACS Appl. Electron. Mater.* **2**, 1352 (2020).
- [19] M. Maruyama, K. Nagashio, and S. Okada, *Phys. Rev. Appl.* **14**, 044028 (2020).
- [20] Y. Gong, J. Lin, X. Wang, G. Shi, S. Lei, Z. Lin, X. Zou, G. Ye, R. Vajtai, B. I. Yakobson, H. Terrones, M. Terrones, B. K. Tay, J. Lou, S. T. Pantelides, Z. Liu, W. Zhou, and P. M. Ajayan, *Nat. Mater.* **13**, 1135 (2014).
- [21] Y. Kobayashi, S. Yoshida, M. Maruyama, H. Mogi, K. Murase, Y. Maniwa, O. Takeuchi, S. Okada, H. Shigekata, and Y. Miyata, *ACS Nano* **13**, 7527 (2019).
- [22] J. Park, J. Lee, L. Liu, K. W. Clark, C. Durand, C. Park, B. G. Sumpter, A. P. Baddorf, A. Mohsin, M. Yoon, G. Gu, and A.-P. Li, *Nat. Commun.* **5**, 5403 (2014).
- [23] H. Zhang, M. Maruyama, Y. Gao, and S. Okada, *Jpn. J. Appl. Phys.* **62**, 025001 (2023).
- [24] A. Kuc, N. Zibouche, and T. Heine, *Phys. Rev. B* **83**, 245213 (2011).
- [25] M. Ye, D. Winslow, D. Zhang, R. Pandey, and Y. K. Yap, *Photonics* **2**, 288 (2015).
- [26] S. Okada and A. Oshiyama, *Phys. Rev. Lett.* **87**, 146803 (2001).
- [27] M. Maruyama, N. Ichinose, Y. Gao, Z. Liu, R. Kitaura, and S. Okada, *ACS Appl. Nano Mater.* **6**, 5434 (2023).
- [28] A.-Y. Lu, H. Zhu, J. Xiao, C.-P. Chuu, Y. Han, M.-H. Chiu, C.-C. Cheng, C.-W. Yang, K.-H. Wei, Y. Yang, Y. Wang, D. Sokaras, D. Nordlund, P. Yang, D. A. Muller, M.-Y. Chou, X. Zhang, and L.-J. Li, *Nat. Nanotechnol.* **12**, 744 (2017).
- [29] J. Zhang, S. Jia, I. Kholmanov, L. Dong, D. Er, W. Chen, H. Guo, Z. Jin, V. B. Shenoy, L. Shi, and J. Lou, *ACS Nano* **11**, 8192 (2017).
- [30] D. B. Trivedi, G. Turgut, Y. Qin, M. Y. Sayyad, D. Hajra, M. Howell, L. Liu, S. Yang, N. H. Patoary, H. Li, M. M. Petrić, M. Meyer, M. Kremser, M. Barbone, G. Soavi, A. V. Stier, K. Müller, S. Yang, I. S. Esqueda, H. Zhuang, J. J. Finley, and S. Tongay, *Adv. Mater.* **32**, 2006320 (2020).
- [31] C. W. Jang, W. J. Lee, J. K. Kim, S. M. Park, S. Kim, and S.-H. Choi, *NPG Asia Mater.* **14**, 15 (2022).
- [32] S. B. Harris, Y.-C. Lin, A. A. Puzos, L. Liang, O. Dyck, T. Berlijn, G. Eres, C. M. Rouleau, K. Xiao, and D. B. Geohegan, *ACS Nano* **17**, 2472 (2023).
- [33] T. Hu, F. Jia, G. Zhao, J. Wu, A. Stroppa, and W. Ren, *Phys. Rev. B* **97**, 235404 (2018).
- [34] W. Zhou, J. Chen, Z. Yang, J. Liu, and F. Ouyang, *Phys. Rev. B* **99**, 075160 (2019).
- [35] Z. Guan, S. Ni, and S. Hu, *J. Phys. Chem. C* **122**, 6209 (2018).
- [36] L. Ju, M. Bie, X. Tang, J. Shang, and L. Kou, *ACS Appl. Mater. Interfaces* **12**, 29335 (2020).
- [37] L. Ju, M. Bie, J. Shang, X. Tang, and L. Kou, *J. Phys. Mater.* **3**, 022004 (2020).
- [38] T. Zheng, Y.-C. Lin, Y. Yu, P. Valencia-Acuna, A. A. Puzos, R. Torsi, C. Liu, I. N. Ivanov, G. Duscher, D. B. Geohegan, Z. Ni, K. Xiao, and H. Zhao, *Nano Lett.* **21**, 931 (2021).
- [39] R. A. Evarestov, A. V. Kovalenko, and A. V. Bandura, *Physica E* **115**, 113681 (2020).
- [40] H.-H. Wu, Q. Meng, H. Huang, C. T. Liud, and X.-L. Wanga, *Phys. Chem. Chem. Phys.* **20**, 3608 (2018).
- [41] S. Oshima, M. Toyoda, and S. Saito, *Phys. Rev. Mater.* **4**, 026004 (2020).
- [42] P. Hohenberg and W. Kohn, *Phys. Rev.* **136**, B864 (1964).
- [43] W. Kohn and L. J. Sham, *Phys. Rev.* **140**, A1133 (1965).
- [44] Y. Morikawa, K. Iwata, and K. Terakura, *Appl. Surf. Sci.* **169-170**, 11 (2001).
- [45] J. P. Perdew, K. Burke, and M. Ernzerhof, *Phys. Rev. Lett.* **78**, 1396 (1997); **77**, 3865 (1996).
- [46] D. Vanderbilt, *Phys. Rev. B* **41**, 7892(R) (1990).
- [47] H. Suzuki, Y. Liu, M. Misawa, C. Nakano, Y. Wang, R. Nakano, K. Ishimura, K. Tsuruta, and Y. Hayashi, *Nano Lett.* **23**, 4533 (2023).
- [48] N. Wada, J. Pu, Y. Takaguchi, W. Zhang, Z. Liu, T. Endo, T. Irisawa, K. Matsuda, Y. Miyauchi, T. Takenobu, and Y. Miyata, *Adv. Funct. Mater.* **32**, 2203602 (2022).
- [49] M. Kaneda, W. Zhang, Z. Liu, Y. Gao, M. Maruyama, Y. Nakanishi, H. Nakajo, S. Aoki, K. Honda, T. Ogawa, K. Hashimoto, T. Endo, K. Aso, T. Chen, Y. Oshima, Y. Yamada-Takamura, Y. Takahashi, S. Okada, T. Kato, and Y. Miyata, *ACS Nano* **18**, 2772 (2024).

- [50] D. H. Robertson, D. W. Brenner, and J. W. Mintmire, *Phys. Rev. B* **45**, 12592(R) (1992).
- [51] S. Sawada and N. Hamada, *Solid State Commun.* **83**, 917 (1992).
- [52] G. Seifert, H. Terrones, M. Terrones, G. Jungnickel, and T. Frauenheim, *Phys. Rev. Lett.* **85**, 146 (2000).
- [53] Y. F. Luo, Y. Pang, M. Tang, Q. Song, and M. Wang, *Comput. Mater. Sci.* **156**, 315 (2019).
- [54] L. Ju, P. Liu, Y. Yang, L. Shi, G. Yang, and L. Sun, *J. Energy Chem.* **61**, 228 (2021).
- [55] Y. Gao and S. Okada, *Appl. Phys. Express* **16**, 075004 (2023).